Nonlinear ultrasound parameter to monitor cell death in cancer cell samples

Pauline Muleki-Seya, Cédric Payan, Laure Balasse, Régine Guillermin, Sandrine Roffino, Benjamin Guillet, and Emilie Franceschini

Citation: The Journal of the Acoustical Society of America **144**, EL374 (2018); doi: 10.1121/1.5066348

View online: https://doi.org/10.1121/1.5066348

View Table of Contents: http://asa.scitation.org/toc/jas/144/5

Published by the Acoustical Society of America

Nonlinear ultrasound parameter to monitor cell death in cancer cell samples

Pauline Muleki-Seya,[1,a)] Cédric Payan,[1,b)] Laure Balasse,[2] Régine Guillermin,[1,b)] Sandrine Roffino,[3,c)] Benjamin Guillet,[2] and Emilie Franceschini[1,b)]

[1]*Aix-Marseille University, CNRS, Centrale Marseille, LMA, Marseille, France*
[2]*Aix Marseille University, INSERM, VRCM, Marseille, France*
[3]*Aix Marseille University, CNRS, ISM, Marseille, France*
pauline.muleki@gmail.com, cedric.payan@univ-amu.fr, laure.balasse@univ-amu.fr, guillermin@lma.cnrs-mrs.fr, sandrine.roffino@univ-amu.fr, benjamin.guillet@univ-amu.fr, franceschini@lma.cnrs-mrs.fr

Abstract: A scaling subtraction method was proposed to analyze the radio frequency data from cancer cell samples exposed to an anti-cancer drug and to estimate a nonlinear parameter. The nonlinear parameter was found to be well correlated ($R^2 = 0.62$) to the percentage of dead cells in apoptosis and necrosis. The origin of the nonlinearity may be related to a change in contacts between cells, since the nonlinear parameter was well correlated to the average total coordination number of binary packings ($R^2 \geq 0.77$). These results suggest that the scaling subtraction method may be used to early quantify chemotherapeutic treatment efficiency.

[CCC]
Date Received: August 3, 2018 **Date Accepted:** October 13, 2018

1. Introduction

Early detection of tumor response to anti-cancer therapy is a major challenge in the fight against cancer. Current methods of assessing therapy effects during patient treatment are often invasive, requiring biopsied tissue or injection of a radioactive substance with functional imaging modalities. The development of a noninvasive method for early detection of tumor response to therapy would thus be of great interest. Contrast ultrasound (US) with microbubbles, a marker of the microvasculature for example, is used in diagnosing a tumor as well as monitoring treatment (Ellegala *et al.*, 2003; Solbiati *et al.*, 2004). Non-invasive quantitative US techniques based on the frequency-based analysis of the signals backscattered from tumors have been successfully used to detect cell death (Brand *et al.*, 2008, 2009; Kolios *et al.*, 2002; Sannachi *et al.*, 2015; Tadayyon *et al.*, 2015) which is a biomarker of tumor response to therapy. The programmed cell death, called apoptosis, is one of the most common cell deaths induced by anti-cancer treatment. During apoptosis, cells undergo significant structural changes: cell shrinkage, DNA fragmentation occurs and nuclei condense and subsequently fragment into apoptotic bodies. These structural changes may lead to changes in contacts between cells. By considering the analogy between a cell pellet and a granular material, a change of contacts between cells could be at the origin of an evolution of the nonlinear component of US scattering (Nesterenko, 1983). The goal of this letter is to assess the ability of a noninvasive nonlinear US approach to monitor response to anti-cancer therapy *in vitro*, as a complement or alternative to standard quantitative US measurement techniques. In a medical application, the quantification of nonlinearity is generally based on the evaluation of the nonlinear tissue parameter B/A (Duck, 2002; Varray *et al.*, 2011). To precisely evaluate the nonlinear parameter, wideband transducers are needed to track the second harmonic component. In nondestructive testing, the microstructural changes in a solid (such as in concrete or rocks) are known to have an influence on non-linear US parameters (Payan *et al.*, 2007) and the Scaling Subtraction Method (SSM) (Bruno *et al.*, 2009; Scalerandi *et al.*, 2008) has been developed to avoid using specific nonlinear equipment. In the present

[a)]Author to whom correspondence should be addressed. Also at: Bioacoustics Research Laboratory, Department of Electrical and Computer Engineering, University of Illinois at Urbana-Champaign, 405 N. Mathews, Urbana, IL 61801, USA.
[b)]Also at: Bioacoustics Research Laboratory, Department of Electrical and Computer Engineering, University of Illinois at Urbana-Champaign, 405 N. Mathews, Urbana, IL 61801, USA.
[c)]Also at: Université de Nice Sophia Antipolis, Nice, France.

work, the SSM was adapted in the frequency domain to estimate the non-linear parameter for cell death monitoring. The SSM was suitable in this study because it was easily applicable with our US system. Ultrasonic measurements were performed at a center frequency of 20 MHz on *in vitro* cell pellet samples (i.e., centrifuged cells). Cell pellets mimic the spatial distribution and packing of cells in tumors and are simplified versions of real tissue since only a single cell line is considered (Franceschini *et al.*, 2014; Kolios *et al.*, 2002). The SSM was applied to differentiate dead from viable cells, and investigate how the nonlinear parameter changes with time or dose upon anti-cancer drug exposure. Finally, this letter studies and discusses the correlation between the nonlinear parameter and the percentage of dead cells.

2. Methods

Experiments were conducted on a human colon adenocarcinoma cell line (HT29) treated with staurosporine, which induces mainly cell apoptosis. The protocol for one cell pellet biophantom preparation is described below. Once cells were grown in T175 flasks, the supernatant (containing dead cells) was removed or reserved, and cells were detached with accutase and washed in phosphate-buffered saline (PBS). Cells from four flasks were collected and the supernatant, if reserved, was added to the collected cells. After homogenization with a pipette tip, 150 and 50 μL of this cell suspension was withdrawn for flow cytometry and for cell size analysis, respectively. The remaining suspension was centrifuged for 5 min at 1200 g and then the medium was aspirated and 500 μL of PBS was added. After homogenization with a pipette tip, the cells were transferred to an 8-well Nunc Lab-Tek II Chamber Slide System (Dominique Dutscher, Brumath, France) and centrifuged for 5 min at 1700 g to form densely-packed cell pellets. The cell pellet samples were submerged in PBS during ultrasonic measurements, and then they were fixed in 10% buffered formalin for 3 days, dehydrated in graded ethanol series, cleared in methylcyclohexane and embedded in methyl methacrylate resin, before being sectioned and stained with toluidine blue.

Different experiment series were conducted to investigate the time-effect or dose-effect of staurosporine on HT29 cell pellets. HT29 cells were treated with 0.5 μM of staurosporine for 0, 6, 12, 24, 36, and 48 h (time effect), or treated for 24 h with different drug doses of 0, 0.125, 0.25, 0.50, 0.75, and 1 μM (dose effect). The dose effect experiments were conducted on cell pellet samples prepared with and without addition of the supernatant at the beginning of the cell pellet preparation, whereas the time effect experiment was conducted on cell pellet samples prepared without addition of the supernatant. Adding the supernatant during the cell pellet preparation allows the percentage of dead cells to be increased.

For each experimental condition, the flow cytometry analysis was realized using Annexin V/7-AAD staining to quantify the percentage of viable (Annexin V -/7-AAD -) and dead cells [apoptosis (Annexin V +/7-AAD - and Annexin V +/7-AAD + for early and late apoptosis, respectively) or necrosis (Annexin V -/7-AAD +)], and the cell diameter distribution was obtained using the Scepter^{TM} 2.0 Cell Counter (Millipore, Darmstadt, Germany). Typical examples of cell diameter distribution for cells treated with staurosporine for 0, 12, and 24 h are shown in Fig. 1(a). The non-treated cells exhibit a unimodal size distribution with a mean cell diameter around 12.9 ± 1.5 μm, whereas the treated cells exhibit a bimodal size distribution with large cells and small cellular fragments. The diameters of the small and large cells were estimated by fitting a mixture of two Gaussian functions on the cell diameter distribution. For each experiment series, the ratio of small diameter to large diameter averaged over the five treated cell pellets was found to be approximately 1:2.6 ($\pm$1:0.4) for the dose effect experiment with supernatant, 1:4.0 ($\pm$1:1.3) the dose effect experiment without supernatant, and 1:3.4 ($\pm$1:0.7) the time effect experiment. The smallest gate diameter D_{LG} sorting small and large cells was determined manually using the non-treated cell size distribution [see the green dotted vertical line in Fig. 1(a)]. Then the volume fraction occupied by small cells Φ_s was defined as

$$\Phi_s = \frac{\int \frac{4}{3}\pi \left(\frac{D < D_{LG}}{2}\right)^3}{\int \frac{4}{3}\pi \left(\frac{D}{2}\right)^3}, \tag{1}$$

where D is the cell diameter. For each experiment series, it was found that the volume fraction occupied by small cells Φ_s was less than 0.34 for the dose effect experiment

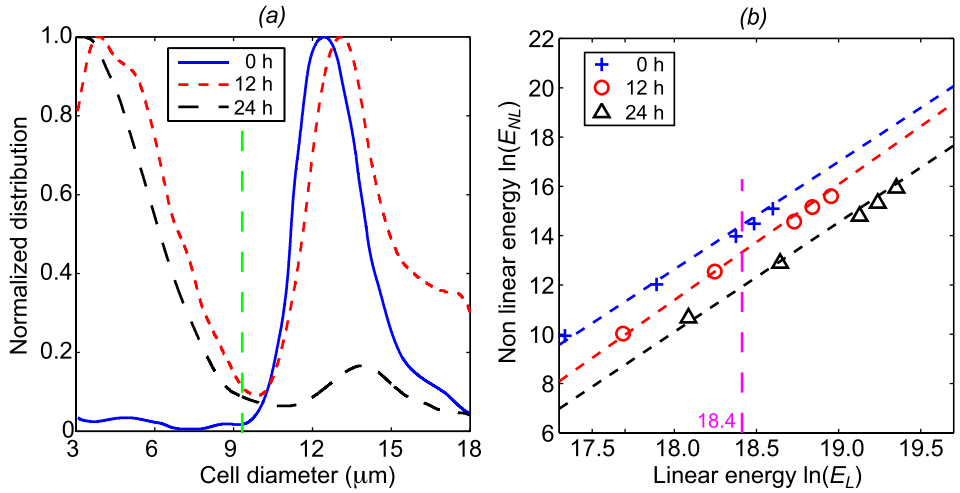

Fig. 1. (Color online) (a) Example of cell diameter distribution for different time exposures (0, 12, and 24 h). The green dotted vertical line corresponds to the smallest gate of the diameters sorting small and large cells. (b) Example of the non-linear energy E_{NL} as a function of the linear energy E_L in a log-log scale (a = 3.98 and b = −59.8).

with supernatant, 0.40 for the dose effect experiment without supernatant, and 0.56 for the time effect experiment.

US measurements were performed on cell pellet samples using a Vevo 770 high frequency US system (Visualsonics Inc., Toronto, Canada) with the RMV 710 probe. An example of a photograph of cell pellet samples probed by the RMV 710 probe is given in Fig. 4 in Franceschini *et al.* (2014). For this probe, the oscillating single-element focused circular transducer had a center frequency of 20 MHz with a −6 dB bandwidth at 10–32 MHz, focuses of 15 mm and *f*-number of 2.1. Radio frequency (RF) data were acquired with this scanner at a sampling frequency of 250 MHz with 8 bit resolution using a Gagescope model CS11G8 acquisition board. For one cell pellet sample, RF data were collected from six different Regions-of-Interest (ROIs, rectangular window covering 1.2 mm axially and 0.5 mm laterally corresponding to 33 adjacent echo lines) using different powers of excitation of the US system: 5%, 10%, 20%, 40%, 50%, and 63% (corresponding to acoustic pressure between 0.64 and 2.29 MPa). An ultrasonic experiment was also performed on a water-agar interface with the RMV710 probe using the different powers of excitation in order to obtain the relationship between the powers as discussed below [see Eq. (2)] and to ensure the linearity of the system for the powers used in this study.

The SSM was adapted in the frequency domain in order to analyze 33 RF signals from ROIs (instead of a single echographic line in the time domain analysis used in Bruno *et al.*, 2009). The modified SSM is described below. The spectra of the RF temporal signals in the ROI were averaged to provide $S_{P_i}(f)$, where i denoted the power of the excitation. The lowest power amplitude $P_{i=5\%}$ was considered to be sufficiently low for the US propagation in the cell pellet sample to behave linearly. Therefore the power spectrum $S_{P_i=5\%}$ represented the linear response of the cell pellet. If the system was linear, the superposition principle would hold true and the output signal at a larger power excitation $P_i > P_{i=5\%}$ would be expected to be

$$S^L_{P_i}(f) = \sqrt{\frac{P_i}{P_{i=5\%}}} S_{P_i=5\%}(f). \tag{2}$$

The reference measurement on water agar interface confirmed the linearity of the system as well as the validity of Eq. (2) with an averaged relative error of 3.8% (data not shown). For each cell pellet, linear and nonlinear parameters (linked to the energy), and denoted linear and nonlinear energy, over the 10–32 MHz frequency bandwidth were defined as

$$E_L(P_i) = \int S^L_{P_i}(f)df \quad \text{and} \quad E_{NL}(P_i) = \int S_{P_i}(f)df. \tag{3}$$

Figure 1(b) represents the nonlinear energy E_{NL} that increases with the linear energy E_L as expected. For each cell pellet (treated or not with the anti-cancer drug), the curve [ln(E_L), ln(E_{NL})] for the different powers was fitted with a one degree polynomial

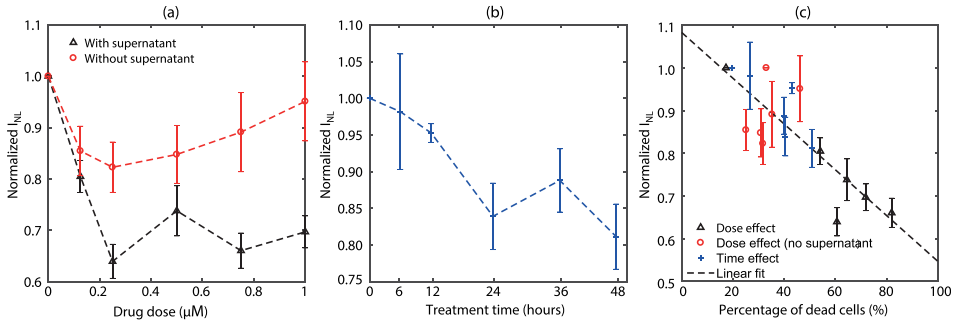

Fig. 2. (Color online) (a) and (b) Normalized I_{NL} parameter as a function of the drug dose (with or without supernatant) and as a function of the drug exposure duration. (c) Correlation between the normalized I_{NL} parameter and the percentage of dead cells (in early and late apoptosis and in necrosis). The error bars represent the standard deviation.

function $\ln(E_{NL}) = a\ \ln(E_L) + b$ [see Fig. 1(b)]. The parameters E_L and E_{NL} were then averaged for the six ROIs. The nonlinear parameter, denoted I'_{NL}, was calculated from the $\ln(E_{NL})$ value on the fitted curve for a given $\ln(E_L)$ value [empirically chosen equal to 18.4 as shown in Fig. 1(b)]. Note that the nonlinear parameter I'_{NL} was previously used to observe damages in concrete (Antonaci *et al.*, 2010). The normalized nonlinear parameter, denoted I_{NL}, corresponds to the I'_{NL} of a treated cell pellet divided by the I'_{NL} of the control (non-treated) cell pellet for each series. The proposed non-linear parameter I_{NL} could be a consequence of either harmonic generation or nonlinear attenuation, or both. The nonlinear parameter linked to the dependence of the elastic constants on amplitude cannot be detected with the proposed SSM in the frequency domain since it results in a phase shift of the temporal excitation signal (Bruno *et al.*, 2009).

3. Results and discussion

The evolution of the normalized I_{NL} parameter as a function of the drug dose and of the drug exposure duration is presented in Figs. 2(a) and 2(b). For both dose effect series, the normalized I_{NL} parameter decreases with increasing doses between 0 and 0.25 μM and then increases or stagnates with increasing doses between 0.25 and 1 μM [Fig. 2(a)]. For the time effect, the normalized I_{NL} parameter decreases overall when the exposure time to the drug increases [Fig. 2(b)]. It is interesting to observe that the I_{NL} parameter varies over a wider range of values for the dose effect experiment when the supernatant is added (i.e., when the proportion of dead cells is larger) ($0.6 \leq I_{NL} \leq 1$), when compared to the time or dose effect experiment without supernatant ($0.76 \leq I_{NL} \leq 1$). The normalized I_{NL} parameter is found to be well correlated to the percentage of apoptotic cells in late or in early and late apoptosis ($R^2 \geq 0.55$, p-value ≤ 0.0001, obtained with the MATLAB function Polyfitn). The best correlation ($R^2 = 0.62$, p-value ≤ 0.0001) is obtained between the normalized I_{NL} parameter and the percentage of dead cells (in apoptosis and in necrosis), as shown by the best linear fit for the three experiment series in Fig. 2(c). Note that the choice of the value on the fitted curve for $\ln(E_L)$ [see Fig. 1(b)] had only a small effect as the slope of the [$\ln(E_L)$, $\ln(E_{NL})$] curves were constants. No correlation was observed between the slope or the offset of the curve [$\ln(E_L)$, $\ln(E_{NL})$] and the percentage of apoptotic or dead cells.

One may argue that the nonlinearity measurement can suffer from the nonlinearity generated by the US propagation in the PBS. However, as the focal position of the probe was always positioned at the same distance from the PBS/cells interface, then between the treated and non-treated cell pellets no nonlinearity due to propagation between the probe and the interface was expected.

In this study, the SSM was adapted in the frequency domain. According to Parseval's theorem, the proposed frequency-based SSM and conventional SSM are identical. However, the use of time series implies introducing the phase of the signals. In experiments, a given RF line has to correspond exactly to the same location on the cell pellet across various powers. If this RF line moves a little bit, the back scattered field would be very different, then the scaled subtraction will result in high nonlinearity, which is not physical. In order to avoid eventual phase cancellation effects induced by non-reproducible RF line positioning, only the magnitude of the Fourier transform is used in this study.

The following discussion intends to determine if the US nonlinearities are generated by an evolution of the contact between cells. The dominant form of cell death

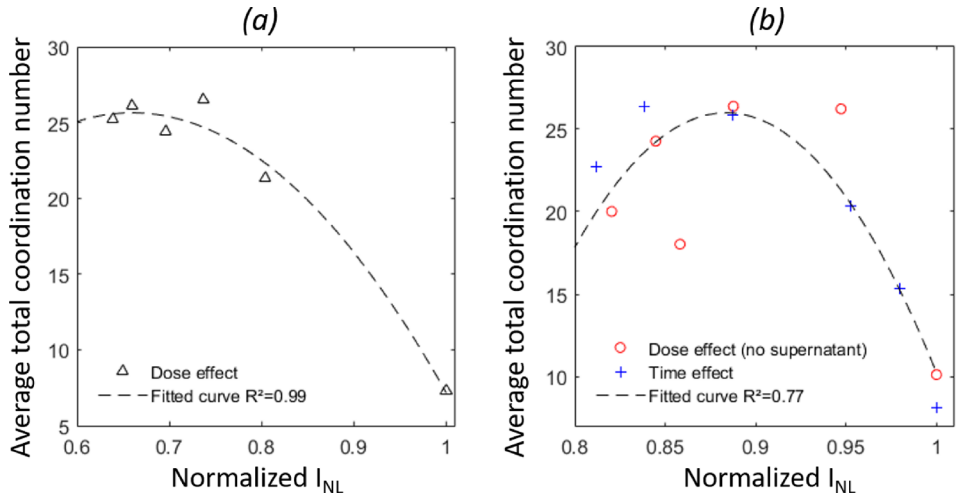

Fig. 3. (Color online) (a) The relationship between the normalized I_{NL} and C for the dose effect experiment with supernatant. (b) The relationship between the normalized I_{NL} and C for the dose effect experiment without supernatant and for the time effect experiment. The dotted lines correspond to the best second order polynomial fit.

in the three experiments was apoptosis: for example, in the dose effect experiment with supernatant, the percentage of apoptotic cells was comprised between 25% and 65%, while the percentage of necrotic cells was comprised between 10% and 30%. During early and late apoptosis and necrosis, morphological changes of cells occur such as cell shrinkage and membrane blebbing during early apoptosis, cell fragmentation during late apoptosis, and cell swelling during necrosis. All these morphological changes may lead to a change in contacts between cells. To confirm this hypothesis, we considered as a first approximation that the cell size distribution is a binary mixture of small and large spheres [as shown previously in Fig. 2(b) with the bimodal size distribution for treated cells]. Based on this approximation, the partial mean coordination numbers between large-large spheres C_{ll}, between large-small spheres C_{ls}, between small-small spheres C_{ss}, and between small-large spheres C_{sl} were computed by assuming that the small-to-large size ratio was equal to 1:2 for the dose effect with supernatant (as its small-to-large cell size ratio was found to be 1:2.6), and assuming that the small-to-large size ratio was equal to 1:4 for the dose effect without the supernatant and for the time effect (as their small-to-large cell size ratios were found to be 1:4.0 and 1:3.4, respectively). This assumption was used in order to compute the partial mean coordination numbers C_{ll}, C_{ls}, C_{ss}, and C_{sl} based on Fig. 5(a) [or Fig. 5(b), respectively] of Pinson *et al.* (1998) for a given volume fraction occupied by small spheres Φ_s for the 1:2 ratio (or the 1:4 ratio, respectively). Finally, the average total coordination number C was estimated as (Dodds and Kuno, 1977),

$$C = [n_l(C_{ll} + C_{ls}) + n_s(C_{ss} + C_{sl})]/(n_l + n_s), \tag{4}$$

where n_l and n_s denote the number of large and small spheres, respectively, for a given volume fraction occupied by small spheres Φ_s. The relationship between the normalized I_{NL} (averaged over the 6 ROIs) and the average total coordination number C is presented in Figs. 3(a) and 3(b). Despite the fact that the average total coordination number used did not correspond exactly to the small-large ratio of cells, a good correlation coefficient ($R^2 \geq 0.77$) was obtained between the normalized I_{NL} and C for the three series of experiments. A linear dependency between I_{NL} and C may have meant that the total number of contacts drives the nonlinear behavior. As it is not the case here, the parabolic trend may say that it is not the total number of contacts C but area of the contacts which drives the nonlinear behavior. This statement is in accordance with the data collected in complex solids such as concrete (Payan *et al.*, 2014) where it is shown that the area of potential contacts scales with the nonlinear parameter rather than the total number of contacts.

4. Conclusions

To conclude, we showed that the non-linear SSM can be used to detect cell death in *in vitro* cell samples. A good correlation ($R^2 = 0.62$) was obtained between the nonlinear parameter and the percentage of dead cells in apoptosis and necrosis. The origin of the nonlinearity might be related to a change in contacts between cells, since the

nonlinear parameter was well correlated to the average total coordination number of binary packings ($R^2 \geq 0.77$). These results indicate the potential of the SSM for using nonlinear US parameters to quantify the degree of cancer cell death and, by extension, to offer promising prospects in view of anti-cancer treatment efficiency monitoring.

Acknowledgments

This work was been carried out thanks to the support of the A*MIDEX project (ANR-11-IDEX-0001-02) funded by the "Investissements d'Avenir" French Government program, managed by the French National Research Agency (ANR).

References and links

Antonaci, P., Bruno, C. L. E., Gliozzi, A. S., and Scalerandi, M. (**2010**). "Evolution of damage-induced nonlinearity in proximity of discontinuities in concrete," Int. J. Solids Struct. **47**(11), 1603–1610.

Brand, S., Solanki, B., Foster, D. B., Czarnota, G. J., and Kolios, M. C. (**2009**). "Monitoring of cell death in epithelial cells using high frequency ultrasound spectroscopy," Ultrasound Med. Biol. **35**(3), 482–493.

Brand, S., Weiss, E. C., Lemor, R. M., and Kolios, M. C. (**2008**). "High frequency ultrasound tissue characterization and acoustic microscopy of intracellular changes," Ultrasound Med. Biol. **34**(9), 1396–1407.

Bruno, C. L. E., Gliozzi, A. S., Scalerandi, M., and Antonaci, P. (**2009**). "Analysis of elastic nonlinearity using the scaling subtraction method," Phys. Rev. B **79**(6), 064108.

Dodds, J., and Kuno, H. (**1977**). "Computer simulation and statistical geometric model for contacts in binary random two-dimensional disk packings," Nature **266**(5603), 614–615.

Duck, F. A. (**2002**). "Nonlinear acoustics in diagnostic ultrasound," Ultrasound Med. Biol. **28**(1), 1–18.

Ellegala, D. B., Leong-Poi, H., Carpenter, J. E., Klibanov, A. L., Kaul, S., Shaffrey, M. E., Sklenar, J., and Lindner, J. R. (**2003**). "Imaging tumor angiogenesis with contrast ultrasound and microbubbles targeted to α v β 3," Circulation **108**(3), 336–341.

Franceschini, E., Guillermin, R., Tourniaire, F., Roffino, S., Lamy, E., and Landrier, J.-F. (**2014**). "Structure factor model for understanding the measured backscatter coefficients from concentrated cell pellet biophantoms," J. Acoust. Soc. Am. **135**(6), 3620–3631.

Kolios, M. C., Czarnota, G. J., Lee, M., Hunt, J. W., and Sherar, M. D. (**2002**). "Ultrasonic spectral parameter characterization of apoptosis," Ultrasound Med. Biol. **28**(5), 589–597.

Nesterenko, V. F. (**1983**). "Propagation of nonlinear compression pulses in granular media," J. Appl. Mech. Tech. Phys. **24**(4), 567–575.

Payan, C., Garnier, V., Moysan, J., and Johnson, P. A. (**2007**). "Applying nonlinear resonant ultrasound spectroscopy to improving thermal damage assessment in concrete," J. Acoust. Soc. Am. **121**(4), EL125–EL130.

Payan, C., Saleh, T., Ulrich, T. J., Le Bas, P. Y., and Guimaraes, M. (**2014**). "Quantitative linear and nonlinear resonance inspection techniques and analysis for material characterization: Application to concrete thermal damage," J. Acoust. Soc. Am. **136**(2), 537–546.

Pinson, D., Zou, R. P., Yu, A. B., Zulli, P., and McCarthy, M. J. (**1998**). "Coordination number of binary mixtures of spheres," J. Phys. D Appl. Phys. **31**(4), 457–462.

Sannachi, L., Tadayyon, H., Sadeghi-Naini, A., Tran, W., Gandhi, S., Wright, F., Oelze, M., and Czarnota, G. J. (**2015**). "Non-invasive evaluation of breast cancer response to chemotherapy using quantitative ultrasonic backscatter parameters," Med. Image Anal. **20**(1), 224–236.

Scalerandi, M., Gliozzi, A., Bruno, C. L. E., Masera, D., and Bocca, P. (**2008**). "A scaling method to enhance detection of a nonlinear elastic response," Appl. Phys. Lett. **92**(10), 101912.

Solbiati, L., Ierace, T., Tonolini, M., and Cova, L. (**2004**). "Guidance and monitoring of radiofrequency liver tumor ablation with contrast-enhanced ultrasound," European J. Radiology **51**, S19–S23.

Tadayyon, H., Sannachi, L., Sadeghi-Naini, A., Al-Mahrouki, A., Tran, W. T., Kolios, M. C., and Czarnota, G. J. (**2015**). "Quantification of ultrasonic scattering properties of in vivo tumor cell death in mouse models of breast cancer," Translational Oncol. **8**(6), 463–473.

Varray, F., Basset, O., Tortoli, P., and Cachard, C. (**2011**). "Extensions of nonlinear b/a parameter imaging methods for echo mode," IEEE Trans. Ultrason., Ferroelectr., Freq. Control **58**(6), 1232–1244.